Electromagnetically induced transparency in rubidium

Abraham J. Olson and Shannon K. Mayer
Department of Physics, University of Portland, Portland, Oregon 97203

(Received 14 March 2008; accepted 29 October 2008)

We investigate ladder-type electromagnetically induced transparency (EIT) in rubidium gas. The theoretical absorption profile of a weak probe laser beam at 780.2 nm ($5S_{1/2} \rightarrow 5P_{3/2}$) is modeled in the presence of a strong coupling laser beam at 776.0 nm ($5P_{3/2} \rightarrow 5D_{5/2}$) and the absorption transparency window is characterized. We use two grating-feedback diode lasers and observe EIT experimentally in rubidium and compare the results to the theory. This experiment brings quantum optics into the advanced undergraduate laboratory and utilizes equipment and expertise commonly available in laboratories equipped to perform diode-laser-based absorption spectroscopy of rubidium. © *2009 American Association of Physics Teachers.*
[DOI: 10.1119/1.3028309]

I. INTRODUCTION

Electromagnetically induced transparency (EIT) is a novel phenomenon used to modify the optical response of an atomic medium to a resonant laser field. In EIT a nonresonant pump field can result in the reduction in the absorption of a weak, resonant probe field, provided the fields are coherently coupled by a common state. Because EIT provides for the active control of the response of a medium to a resonant light field, it offers a unique means of coherently controlling photons and holds great promise for fields such as quantum computing and telecommunications.

Electromagnetically induced transparency was first observed in 1991 using high-power pulsed lasers in strontium vapor.[1] Later experiments were done using continuous sources in vapor cells, atomic beams, magneto-optic traps, and Bose-Einstein condensates. We refer readers to the comprehensive topical reviews by Marangos[2] and Fleischhauer *et al.*[3] Fundamental and commercial applications of EIT in atomic physics and quantum optics include lasing without population inversion,[4] reduction of the speed of light (slow light),[5] quantum memory,[6] optical switches,[7,8] all-optical wavelength converters[9] for telecommunications, and quantum information processing.[10] Clarke *et al.*[8] have used EIT in a rubidium ladder system to create an optical switch that can change at rates up to 1 MHz.

A classical analog of EIT that is useful experimentally consists of two coupled RLC circuits.[11] Electromagnetically induced transparency and the closely related topic of coherent population trapping is also the focus of Ref. 12. The rubidium experiment presented here complements and extends this work by allowing students to directly observe and characterize EIT in an atomic system using grating-feedback diode lasers.

Grating-feedback diode laser systems provide reliable, tunable (5–10 GHz), narrow-band (<1 MHz) laser light. Low-cost systems have been developed that are suitable for construction by undergraduates,[13–16] making possible a wide range of experiments in atomic physics.[17–21] Diode laser systems provide sufficient optical power (10–80 mW for the laser systems in Refs. 13–16) to make possible experiments more typically done using high-power laser systems such as two-photon spectroscopy[22] and EIT.

Doppler-free saturated absorption spectroscopy is a simple experiment often performed using a tunable diode laser tuned to the $5S_{1/2} \rightarrow 5P_{3/2}$ D_2 line in rubidium ($\lambda = 780.24$ nm).[13,23] The experiment introduces students to basic laser absorption spectroscopy and allows them to investigate atomic energy levels, hyperfine structure features, and the effect of a Doppler shift on atomic spectra. Two-photon spectroscopy of rubidium[22] using the $5S_{1/2} \rightarrow 5D_{5/2}$ transition ($\lambda = 778.1$ nm) allows for the simultaneous observation of Doppler-free and Doppler-broadened fluorescence spectra from which the hyperfine levels of rubidium can be resolved. The experiment presented here uses much of the same equipment as the single- and two-photon experiments in rubidium and can be easily implemented by laboratories with the apparatus for these experiments.

In this paper we describe the relevant theory, present theoretical and experimental results for ladder-type EIT in rubidium, and describe the experimental procedure and equipment.[24]

II. THEORY

The term electromagnetically induced transparency was coined in a 1990 paper by Harris *et al.*[25] They showed that when a strong coupling laser field is used to drive a resonant transition in a three-level atomic system, the absorption of a weak probe laser field can be reduced or eliminated, provided that the two resonant transitions are coherently coupled to a common state. Shortly thereafter, they reported the first observation of EIT in a strontium gas vapor.[1] The initial research by Harris and his collaborators is now referred to as lambda-type EIT, where two low-level energy states are coupled to a common excited state. The use of the term EIT has since broadened to include V-type and ladder-type configurations. Figure 1 shows the different energy levels and transitions used in the three configurations of EIT. Conventions vary, but we will use the $|1\rangle \rightarrow |3\rangle$ transition for the dipole forbidden (nondipole coupled) transition for all types.

In EIT two laser beams, designated coupling (ω_C) and probe (ω_P), are used to excite electronic transitions in the atoms. The strong coupling laser is used to couple the $|2\rangle \rightarrow |3\rangle$ states such that a probe laser tuned to the $|1\rangle \rightarrow |2\rangle$ transition passes through the medium without being absorbed. Although lambda-type EIT may have the most promise for commercial applications because of the easier achievement of complete transparency on the D_1 line in rubidium, ladder-type EIT has also been used for basic research because the EIT transitions in rubidium are readily

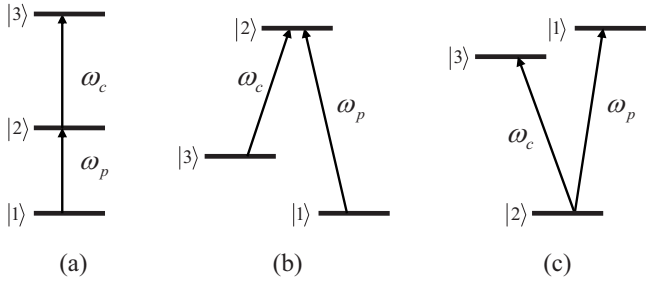

Fig. 1. Three configurations for EIT: (a) ladder; (b) lambda; and (c) V. The frequencies ω_c and ω_p correspond to the coupling and probe laser frequencies, respectively.

accessible using low-power coupling diode lasers. Ladder-type EIT is the focus of the theoretical and experimental work presented here.

The energy level diagram shown in Fig. 2 shows the relevant transitions for ladder-type EIT in rubidium. The $5S_{1/2} \rightarrow 5P_{3/2}$ transition at 780.2 nm (vacuum wavelength) serves as the probe transition. The $5P_{3/2} \rightarrow 5D_{5/2}$ transition at 776.0 nm serves as the coupling transition. The hyperfine splitting of the $5S_{1/2}$ ground state (~GHz) is greater than the Doppler broadening of the transition (~510 MHz) in room temperature rubidium. The hyperfine energy splitting of the $5P_{3/2}$ state (~MHz) is within the Doppler width. This splitting does not impact the experiment because it is the two-photon resonance that is important.[26] The hyperfine energy splitting of the $5D_{5/2}$ state is relevant, and the energy levels are shown in the expanded view to the right in Fig. 2. Electrons in the $5D_{5/2}$ state can return to the ground state through the $5P_{3/2}$ state or via $5D \rightarrow 6P \rightarrow 5S$ cascade decay, emitting 420 nm light.

The theory for lambda, ladder, V-type, and two-photon EIT has been well documented (see Refs. 2 and 3 and references therein). Gea-Banacloche *et al.* have presented a simplified theoretical model for EIT in a rubidium ladder system.[27] Our theoretical development summarizes the salient features of their work. Their approach follows a standard semiclassical analysis in which the laser fields are treated classically and the atoms are modeled quantum mechanically. Interested readers are referred to Refs. 28 and 29 for a discussion of the semiclassical theory of atom-field interactions. A fully quantized model of EIT for single photons is in Ref. 30.

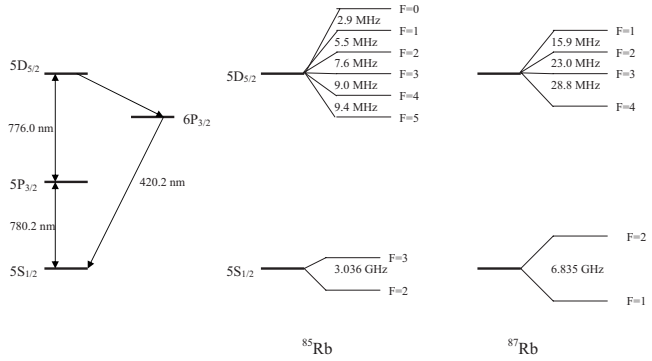

Fig. 2. Energy level diagram for rubidium. The relevant hyperfine levels for ^{85}Rb and ^{87}Rb are shown in the expanded view on the right-hand side.

The optical response of the medium to the probe laser field is characterized by the absorption and dispersion characteristics of the medium and can be obtained from the real and imaginary parts of the complex susceptibility $\chi = \chi' + i\chi''$. The absorption coefficient is given by

$$\alpha = \frac{\omega_p n_0 \chi''}{c}, \tag{1}$$

and the dispersion coefficient is given by

$$\beta = \frac{\omega_p n_0 \chi'}{2c}, \tag{2}$$

where n_0 is the background index of refraction and c is the speed of light.

To determine the complex susceptibility we analyze the density matrix for the three-level system. The on-diagonal density matrix elements ρ_{ij} correspond to the probability of being in a particular state, and the off-diagonal elements are proportional to the electric-dipole moment of the transition and describe the coherence associated with the transition. The density matrix elements are calculated from the Liouville (or Von Neumann) equation of motion[28]

$$\dot{\rho} = -\frac{i}{\hbar}[H, \rho]. \tag{3}$$

For the EIT-ladder system the coupled equations are given by[27]

$$\dot{\rho}_{32} = -(\gamma_{32} - i\Delta_2)\rho_{32} + ig_{32}E_c(\rho_{33} - \rho_{22}) + ig_{21}E_p^*\rho_{31}, \tag{4a}$$

$$\dot{\rho}_{21} = -(\gamma_{21} - i\Delta_1)\rho_{21} + ig_{21}E_p(\rho_{22} - \rho_{11}) - ig_{32}E_c^*\rho_{31}, \tag{4b}$$

$$\dot{\rho}_{31} = -[\gamma_{31} - i(\Delta_1 + \Delta_2)]\rho_{31} - ig_{32}E_c\rho_{21} + ig_{21}E_p\rho_{32}. \tag{4c}$$

The decay rates, γ_{ij}, are related to the natural decay rates of the states, Γ_i, by the relation $\gamma_{ij} = (\Gamma_i + \Gamma_j)/2$. The natural decay rate of the ground state Γ_1 is zero, $\Gamma_2/2\pi$ is 6 MHz, and $\Gamma_3/2\pi$ is 0.97 MHz. The probe laser is denoted by ω_P, and its detuning from the $|1\rangle \rightarrow |2\rangle$ transition frequency ω_{12} is given by Δ_1. The coupling laser is denoted by ω_c, and its detuning from the $|2\rangle \rightarrow |3\rangle$ transition frequency ω_{23} is Δ_2. The coupling and probe field amplitudes are E_c and E_p, respectively. The dipole moment matrix elements for the transitions are $2\hbar g_{ji}$. The Rabi frequency of the coupling laser field is $\Omega_c = 2g_{32}E_c$.

If we solve Eq. (4) in steady state ($\dot{\rho} = 0$), neglect the population of states $|2\rangle$ and $|3\rangle$ (that is, $\rho_{22} \approx \rho_{33} \approx 0$, $\rho_{11} \approx 1$), and assume only the coupling field is strong, the solutions for ρ_{31} and ρ_{21} can be approximated as

$$\rho_{31} \approx -\frac{ig_{32}E_c}{\gamma_{31} - i(\Delta_1 + \Delta_2)}\rho_{21}, \tag{5}$$

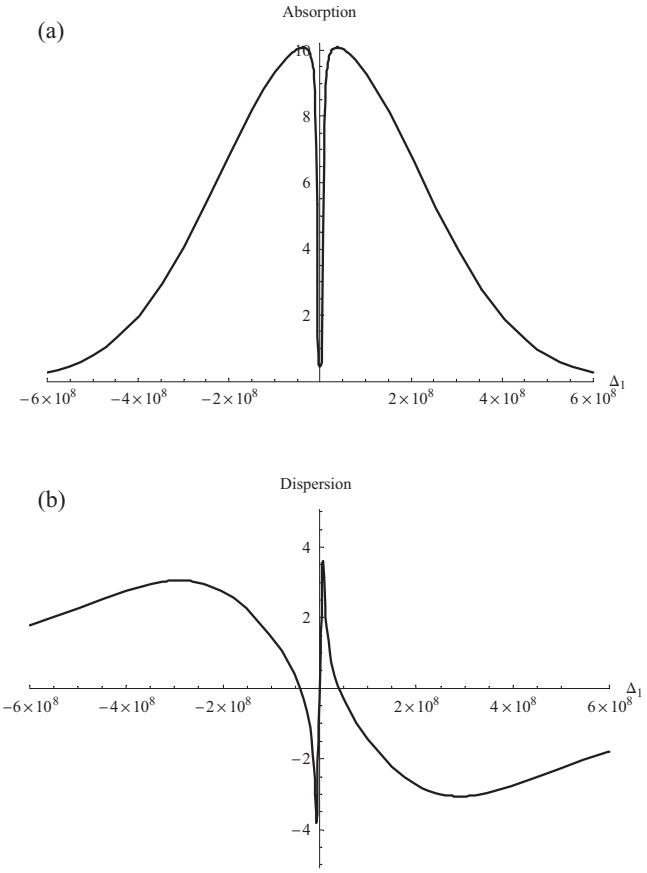

Fig. 3. Theoretical curves for the (a) absorption and (b) dispersion of the probe beam. The coupling laser detuning Δ_2 is zero and the Rabi frequency Ω_c is 80 MHz.

$$\rho_{21} \approx -\frac{ig_{21}E_p}{\gamma_{21} - i\Delta_1 + \dfrac{\Omega_c^2/4}{\gamma_{31} - i(\Delta_1 + \Delta_2)}}. \tag{6}$$

The matrix element ρ_{31} corresponds to the coherence that develops between states $|3\rangle$ and $|1\rangle$ due to the presence of the two laser fields driving the resonant $|1\rangle \rightarrow |2\rangle$ and $|2\rangle \rightarrow |3\rangle$ transitions. The matrix element ρ_{21} yields information about the transition rate at the probe frequency and is clearly impacted by the intensity and detuning of the nonresonant coupling laser. The matrix element ρ_{21} is related to the complex susceptibility by the polarization relation,

$$P = \frac{1}{2}\varepsilon_0 E_p[\chi(\omega_p)e^{-i\omega_p t} + \text{c.c.}] = -2\hbar g_{21} N \rho_{21} e^{-i\omega_p t} + \text{c.c.}, \tag{7}$$

where N is the density of atoms and c.c. is the complex conjugate.

We substitute ρ_{21} from Eq. (6) into Eq. (7) and include the effects of Doppler broadening (see Ref. 27) and calculate the absorption and dispersion of the gas. The results can be graphed using software such as MATHEMATICA and the absorption and dispersion characteristics of the medium can be investigated as a function of the adjustable parameters (for example, Ω_c and Δ_2).

Figure 3 shows the theoretical absorption and dispersion curves when the coupling laser is on resonance with the $|2\rangle \rightarrow |3\rangle$ transition and the coupling laser Rabi frequency is 80 MHz. The EIT transparency window is clearly evident in the absorption curve shown in Fig. 3(a). Figure 3(b) shows the dispersion curve. The dispersion is related to the index of refraction of the gas. The rapidly changing dispersive curve at the EIT resonance point is a characteristic of EIT phenomena and is responsible for the reported slowing of light associated with EIT.[5] We did not characterize the dispersion curve experimentally.

Figure 4 shows the effect of strengthening the coupling laser field and reveals the Aulter-Townes splitting[31] present at strong coupling field strengths. The absorption and dispersion curves from this atomic system correspond to those generated from analysis of the classical analog of EIT (mass-spring system) done in Ref. 11.

III. EXPERIMENTAL APPARATUS

A diagram of the experimental apparatus is shown in Fig. 5. The main components are two grating-feedback diode lasers and accompanying optics, a rubidium vapor cell, and the detection apparatus for absorption and fluorescence (optional). The laser systems were hand-built, grating-feedback, extended-cavity diode lasers operating in a Littrow configuration.[14] The laser diodes were Hitachi model HL 78516, specified to provide nominally 50 mW of optical power with a typical free-running wavelength of approximately 785 nm. The laser injection current was provided by a low-noise current control circuit.[32] The diode lasers were each temperature stabilized using a proportional, integral, and differential feedback circuit[33] to regulate the current through a Peltier element located under the laser mount. Details regarding building grating-feedback laser systems are found in Refs. 13–16. Tunable diode lasers, current control circuits, and temperature control circuits with similar characteristics are also commercially available.[34]

The laser beams were nominally linearly polarized upon exiting the lasers, with a vertical plane of polarization. An aperture, centered on the laser output, provided a circular beam profile. The coupling laser beam was sent through a polarizing beamsplitter cube, which was oriented to transmit vertical polarization, and then focused into the rubidium cell using a 150 mm focal length lens. This setup provided approximately 25 mW of coupling laser power at the cell. The probe laser beam was first attenuated with an aperture that narrowed the beam width and attenuated the power to approximately 500 μW. A 90/10 beamsplitter diverted a portion of the beam to a second rubidium cell and onto a silicon photodetector, which provided a frequency reference. The polarization of the probe laser beam was rotated to the horizontal plane using a quarter-wave plate and linear polarizer (a half-wave plate could be used). The intensity of the probe laser was controlled using neutral density filters. The probe laser beam was focused onto the rubidium cell using a 150 or 80 mm focal length lens. The polarization configuration of the probe laser beam allowed it to be separated by the polarizing beamsplitter after the cell and sent to a photodetector to monitor absorption using a ThorLabs Det210 silicon photodetector.

The 100 mm long rubidium vapor cell from Opthos Instruments had optical quality windows and contained natural rubidium (72% ^{85}Rb, 28% ^{87}Rb). It was used at room temperature. The coupling and probe laser beams were aligned to counterpropagate through the rubidium cell. During the ini-

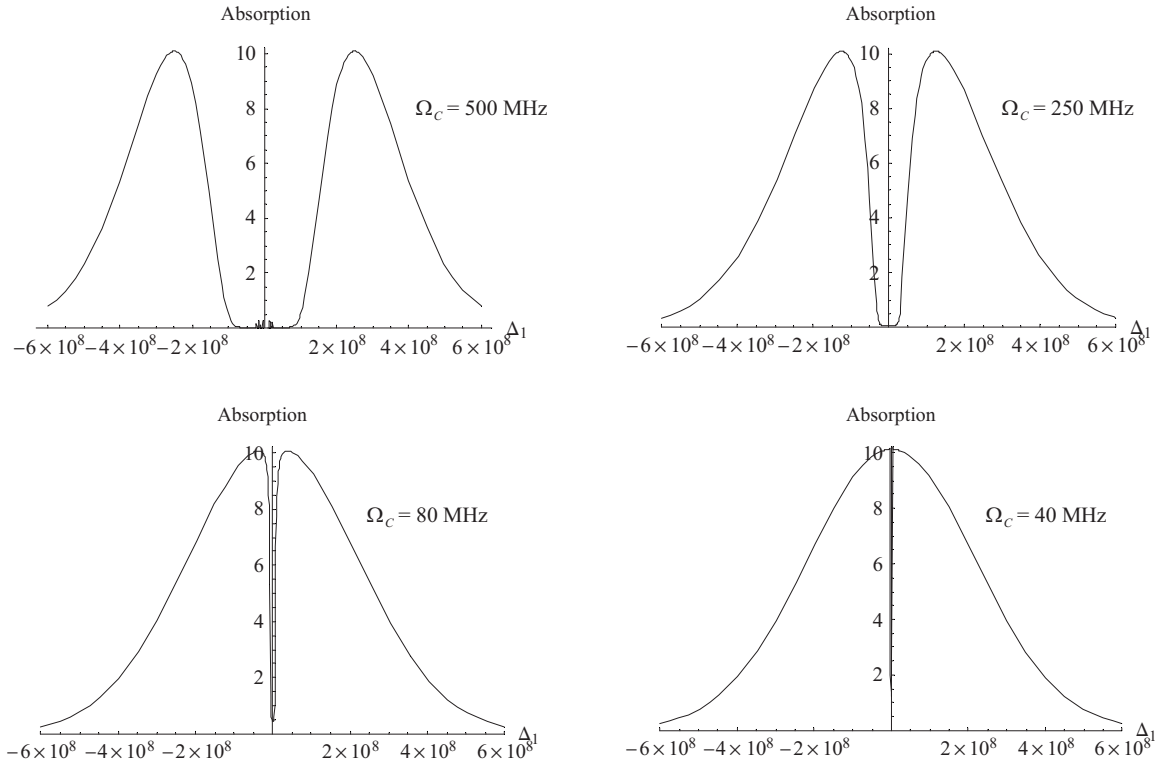

Fig. 4. Theoretical absorption spectra for various coupling laser strengths and zero coupling laser detuning.

tial alignment the adjustable apertures following the lasers were stopped down to ensure maximum overlap of the centers of the counterpropagating beams.

The fixed frequency of the coupling laser was set to the $5P_{3/2} \rightarrow 5D_{5/2}$ transition wavelength by adjusting the temperature and current. The frequency of the probe laser beam was scanned by approximately 3 GHz across the $5S_{1/2} \rightarrow 5P_{3/2}$ Doppler-broadened absorption profile by driving a piezoelectric transducer in the flexure of the laser assembly. The laser wavelengths were monitored using a Burleigh WA-2500 Wavemeter$_{\text{Jr}}$ wavelength meter.

While the Doppler-broadened absorption profile of the probe laser beam was monitored, the fluorescence spectrum was simultaneously monitored (optional) using a Burle 931A photomultiplier tube, with a 420 nm interference filter in place. The photomultiplier tube was placed perpendicular to the axis of beam propagation. Both the absorption and fluorescence signals were recorded via a digital oscilloscope and computer for different combinations of the coupling and probe laser intensity and beam alignment and focusing.

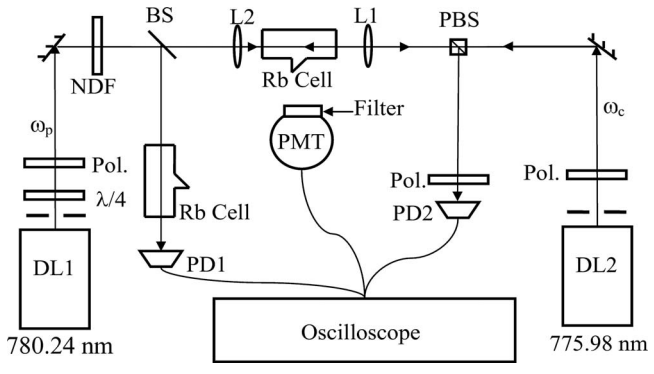

Fig. 5. Apparatus for the ladder-type EIT experiment. Components include grating-feedback diode lasers (DL), quarter-wave plates ($\lambda/4$), linear polarizers (Pol), neutral density filter (NDF), beamsplitter (BS), polarizing beam splitter (PBS), lenses (L), rubidium cells, and photodetectors (PD). The fluorescence detection equipment (optional) includes a 420 nm interference filter and photomultiplier tube (PMT).

IV. EXPERIMENTAL RESULTS AND DISCUSSION

Sample Doppler-broadened absorption spectra with EIT features are shown in Fig. 6 for different coupling laser strengths. Only the first two absorption lines are shown. The corresponding fluorescence signals are shown in Fig. 7. The hyperfine features of the $5D_{5/2}$ state are clearly visible in the absorption and fluorescence spectra for ^{87}Rb. The data were

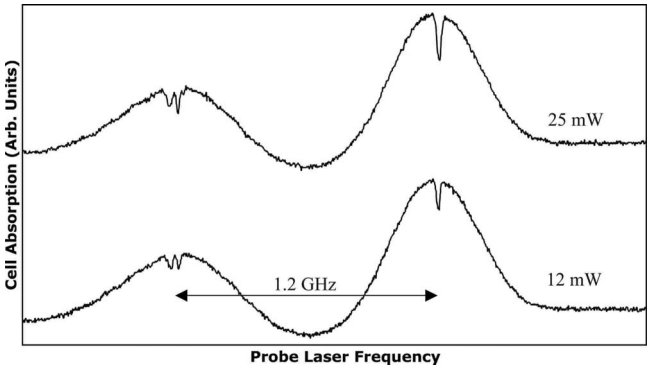

Fig. 6. Doppler-broadened absorption peaks with EIT features. The peak on the left [right] originates from the ^{87}Rb $F_g=2$ [^{85}Rb $F_g=3$] energy state. Spectra were taking using coupling lasers powers of 12 and 25 mW.

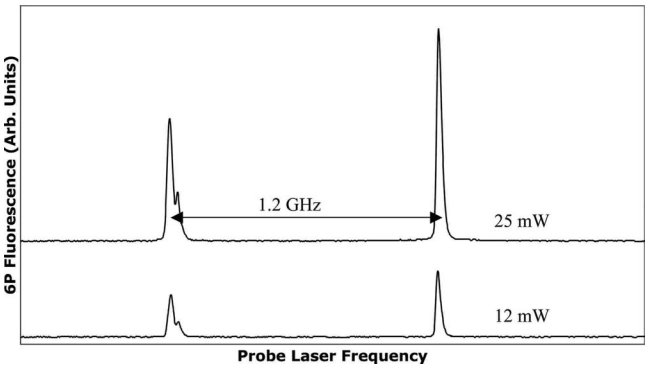

Fig. 7. Fluorescence spectra from the $5D \rightarrow 6P \rightarrow 5S$ cascade decay. The peak on the left [right] originates from the ^{87}Rb $F_g=2$ [^{85}Rb $F_g=3$] energy state. Spectra were taking using coupling laser powers of 12 and 25 mW.

taken with a 550 μW unfocused probe laser beam. The EIT window is evident in the spectra in Fig. 6. The transmission increased from 22% to 34% for ^{85}Rb when the coupling laser power was increased from 12 to 25 mW.

Quantitative comparison with our theoretical result is complicated due to the uncertainty in determining the coupling laser Rabi frequency[27] and the omission of the hyperfine structure of the $5D_{5/2}$ state in the theoretical model. Our experimental results show qualitative agreement with our theoretical absorption profiles for low coupling laser power. As predicted, the effect of increasing the coupling laser power clearly increased the EIT effect, although the power was not sufficient to observe the Aulter-Townes splitting predicted theoretically for higher coupling laser power and seen by others experimentally.[35]

Figure 8 shows an expanded view of the EIT features in the absorption spectra and corresponding fluorescence spectra for ^{87}Rb and ^{85}Rb. The hyperfine splitting of the $5D_{5/2}$ state is clearly resolvable in the fluorescence spectra. Badger *et al.*[36] have studied the effects of hyperfine splitting on the EIT absorption profile and found that hyperfine splitting on the order of or greater than the Rabi frequency of the coupling laser beam results in a noticeable broadening of the transparency window [Fig. 8(b)] or even distinct peaks in the absorption profile [Fig. 8(a)]. Moseley *et al.*[35] have proposed the use of EIT resonances for spectroscopy of two-photon transitions. The hyperfine features observed in the Fig. 8 spectra were analyzed and found to have structure corresponding to that characterized in the two-photon spectroscopy laboratory by Olson *et al.*[22]

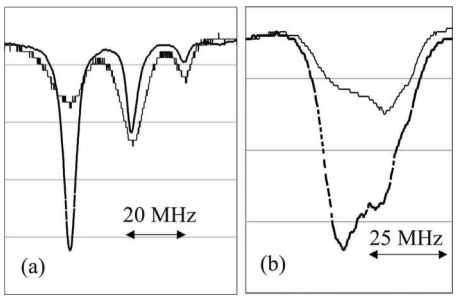

Fig. 8. An expanded view of the hyperfine features of EIT in the absorption spectra (solid) and corresponding fluorescence spectra (dashed) for (a) ^{87}Rb and (b) ^{85}Rb. The fluorescence spectra are inverted for clarity. The vertical scale is relative. The resolved peaks in the ^{87}Rb spectra correspond to the $F=4$, $F=3$, and $F=2$ hyperfine levels of the $5D_{5/2}$ state.

Other research groups have reported EIT behavior using the same rubidium ladder system we have employed (see, for example, Refs. 26, 27, 35, 37, and 38). Our experimental conditions are most similar to those of Xiao *et al.*[37] They used two diode lasers and a room-temperature rubidium cell and reported a 52.5% reduction in absorption for a coupling beam power of 20 mW. A key difference of our experiment is the lack of magnetic shielding, which can result in a Zeeman shift in the rubidium energy levels. The magnetic field recorded in the region of our rubidium cell was 0.18–0.24 mT, corresponding to a Zeeman shift of approximately 8 MHz. Fulton *et al.* cite Zeeman splitting and Stark shifting of the $5P$ and $5D$ states as contributing causes to a reduction in the occurrence of EIT.[26] We anticipate that improved optimization of the laser focus, alignment, and intensity would also result in an increase in the depth of the transparency window. Further improvements could be achieved by electronically frequency-locking the coupling laser.

V. SUMMARY

We have described an EIT experiment using rubidium atoms that is suitable for the advanced undergraduate laboratory. The theoretical absorption profile of a weak probe laser beam is modeled in the presence of a strong coupling laser beam and the absorption window is characterized. By using two grating-feedback diode lasers we achieved a 34% reduction in absorption using a relatively low-power coupling laser beam. This work complements and extends the analysis of EIT-like behavior in a classical system[11] by allowing students to directly observe and characterize EIT in an atomic medium. Moreover, it provides laboratories equipped to perform absorption spectroscopy of rubidium with a novel opportunity to investigate coherent phenomena.

ACKNOWLEDGMENTS

The authors acknowledge the support of the M. J. Murdock Charitable Trust and the University of Portland.

[1] K. J. Boller, A. Imamoglu, and S. E. Harris, "Observation of electromagnetically induced transparency," Phys. Rev. Lett. **66**, 2593–2596 (1991).
[2] J. P. Marangos, "Electromagnetically induced transparency," J. Mod. Opt. **45**, 471–503 (1998).
[3] M. Fleischhauer, A. Imamoglu, and J. Marangos, "Electromagnetically induced transparency: Optics in coherent media," Rev. Mod. Phys. **77**, 633–673 (2005).
[4] O. Kocharovskaya, "Amplification and lasing without inversion," Phys. Rep. **219**, 175–190 (1992).
[5] L. V. Hau, S. E. Harris, Z. Dutton, and C. H. Behroozi, "Light speed reduction to 17 meters per second in an ultracold atomic gas," Nature (London) **397**, 594–598 (1999).
[6] M. D. Lukin, S. F. Yelin, and M. Fleischhauer, "Entanglement of atomic ensembles by trapping correlated photon states," Phys. Rev. Lett. **84**, 4232–4235 (2000).
[7] S. E. Harris and Y. Yamamoto, "Photon switching by quantum interference," Phys. Rev. Lett. **81**, 3611–3614 (1998).
[8] J. Clarke, H. Chen, and W. A. van Wijngaarden, "Electromagnetically induced transparency and optical switching in a rubidium cascade system," Appl. Opt. **40**, 2047–2051 (2001).
[9] H. Schmidt and R. J. Ram, "All-optical wavelength converter and switch based on electromagnetically induced transparency," Appl. Phys. Lett. **76**, 3173–3175 (2000).
[10] R. G. Beausoleil, W. J. Munro, D. A. Rodrigues, and T. P. Spiller, "Ap-

plications of electromagnetically induced transparency to quantum information processing," J. Mod. Opt. **51**, 2441–2448 (2004).
[11] C. L. Garrido Alzar, M. A. G. Martinez, and P. Nussenzveig, "Classical analog of electromagnetically induced transparency," Am. J. Phys. **70**, 37–41 (2002).
[12] T. Pang, "Electromagnetically induced transparency," Am. J. Phys. **69**, 604–606 (2001).
[13] K. B. MacAdam, A. Steinbach, and C. Wieman, "A narrow-band tunable diode laser system with grating feedback, and a saturated absorption spectrometer for Cs and Rb," Am. J. Phys. **60**, 1098–1110 (1992).
[14] J. J. Maki, N. S. Campbell, C. M. Grande, R. P. Knorpp, and D. H. McIntyre, "Stabilized diode-laser system with grating feedback and frequency-offset locking," Opt. Commun. **102**, 251–256 (1993).
[15] A. S. Arnold, J. S. Wilson, and M. G. Boshier, "A simple extended-cavity diode laser," Rev. Sci. Instrum. **69**, 1236–1239 (1998).
[16] R. S. Conroy, A. Carleton, A. Carruthers, B. D. Sinclair, C. F. Rae, and K. Dholakia, "A visible extended cavity diode laser for the undergraduate laboratory," Am. J. Phys. **68**, 925–931 (2000).
[17] C. Leahy, J. T. Hastings, and P. M. Wilt, "Temperature dependence of Doppler-broadening in rubidium: An undergraduate experiment," Am. J. Phys. **65**, 367–371 (1997).
[18] G. N. Rao, M. N. Reddy, and E. Hecht, "Atomic hyperfine structure studies using temperature/current tuning of diode lasers: An undergraduate experiment," Am. J. Phys. **66**, 702–712 (1998).
[19] D. A. Van Baak, "Resonant Faraday rotation as a probe of atomic dispersion," Am. J. Phys. **64**, 724–735 (1996).
[20] K. G. Libbrecht, R. A. Boyd, P. A. Willems, T. L. Gustavson, and D. K. Kim, "Teaching physics with 670 nm diode lasers-construction of stabilized lasers and lithium cells," Am. J. Phys. **63**, 729–737 (1995).
[21] M. Terrell and M. F. Masters, "Laser spectroscopy of the cesium dimer as a physics laboratory experiment," Am. J. Phys. **64**, 1116–1120 (1996).
[22] A. J. Olson, E. J. Carlson, and S. K. Mayer, "Two-photon spectroscopy of rubidium using a grating-feedback diode laser," Am. J. Phys. **74**, 218–223 (2006).
[23] J. R. Brandenburger, *Lasers and Modern Optics in Undergraduate Physics* (Lawrence U. P., Appleton, WI, 1991), pp. 49–59.
[24] The identification of commercial suppliers and part numbers is given to provide sufficient detail. This identification is not intended as an endorsement or recommendation of these particular suppliers. Alternate suppliers might provide similar equipment that meets or exceeds the performance of the equipment listed.
[25] S. E. Harris, J. E. Field, and A. Imamoglu, "Nonlinear optical processes using electromagnetically induced transparency," Phys. Rev. Lett. **64**, 1107–1114 (1990).
[26] D. J. Fulton, R. R. Moseley, S. Shepherd, B. D. Sinclair, and M. H. Dunn, "Effects of Zeeman splitting on electromagnetically-induced transparency," Opt. Commun. **116**, 231–239 (1995).
[27] J. Gea-Banacloche, Y. Li, S. Jin, and M. Xiao, "Electromagnetically induced transparency in ladder-type inhomogeneously broadened media: Theory and experiment," Phys. Rev. A **51**, 576–584 (1995).
[28] M. O. Scully and M. S. Zubairy, *Quantum Optics* (Cambridge U. P., Cambridge, 1997).
[29] M. Sargent, III, M. O. Scully, and W. E. Lamb, Jr., *Laser Physics* (Addison-Wesley, Reading, MA, 1974).
[30] T. Purdy and M. Ligare, "Electromagnetically induced transparency and reduced speeds for single photons in a fully quantized model," J. Opt. B: Quantum Semiclassical Opt. **5**, 289–299 (2003).
[31] S. H. Autler and C. H. Townes, "Stark effect in rapidly varying fields," Phys. Rev. **100**, 703–722 (1955).
[32] A. Hemmerich, D. H. McIntyre, D. Schropp, Jr., D. Meschede, and T. W. Hänsch, "Optically stabilized narrow linewidth semiconductor laser for high resolution spectroscopy," Opt. Commun. **75**, 118–122 (1990).
[33] C. C. Bradley, J. Chen, and R. G. Hulet, "Instrumentation for stable operation of laser diodes," Rev. Sci. Instrum. **61**, 2097–2101 (1990).
[34] Examples include New Focus Tunable Laser TLB-6312, Thor Labs tunable laser TL780-T, Thor Labs laser diode current controller LDC201U, and Thor Labs temperature controller TED200.
[35] R. R. Moseley, S. Shepherd, D. J. Fulton, B. D. Sinclair, and M. H. Dunn, "Two-photon effects in continuous-wave electromagnetically-induced transparency," Opt. Commun. **119**, 61–68 (1995).
[36] S. D. Badger, I. G. Hughes, and C. S. Adams, "Hyperfine effects in electromagnetically induced transparency," J. Phys. B **34**, L749–L756 (2001).
[37] M. Xiao, Y. Li, S. Jin, and J. Gea-Banacloche, "Measurement of dispersive properties of electromagnetically induced transparency in rubidium atoms," Phys. Rev. Lett. **74**, 666–669 (1995).
[38] J. H. Xu, G. C. La Rocca, F. Bassani, D. Wang, and J. Y. Gao, "Electromagnetically induced one-photon and two-photon transparency in rubidium atoms," Opt. Commun. **216**, 157–164 (2003).